Article

Non-Arrhenius Behavior in the Unfolding of a Short, Hydrophobic □-Helix. Complementarity of Molecular Dynamics and Lattice Model Simulations

Olivier Collet, and Christophe Chipot

J. Am. Chem. Soc., **2003**, 125 (21), 6573-6580• DOI: 10.1021/ja029075o • Publication Date (Web): 01 May 2003

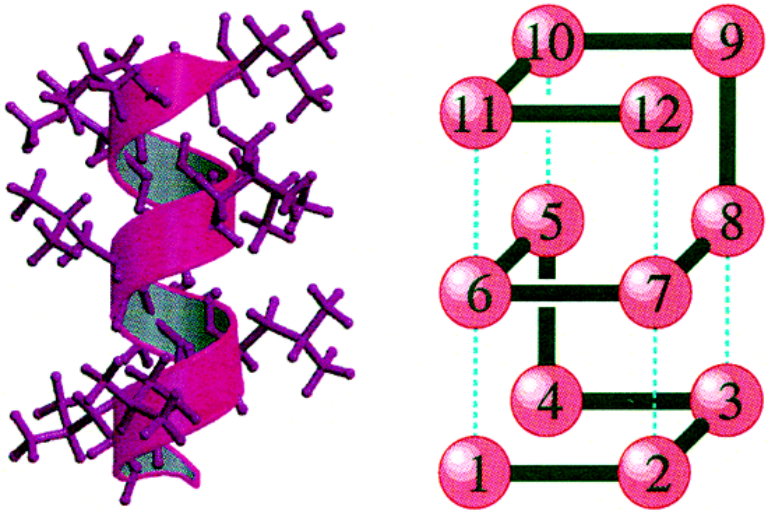

More About This Article

Additional resources and features associated with this article are available within the HTML version:

- Supporting Information
- Access to high resolution figures
- Links to articles and content related to this article
- Copyright permission to reproduce figures and/or text from this article

View the Full Text HTML

J|A|C|S
ARTICLES
Published on Web 05/01/2003

Non-Arrhenius Behavior in the Unfolding of a Short, Hydrophobic α-Helix. Complementarity of Molecular Dynamics and Lattice Model Simulations

Olivier Collet* and Christophe Chipot*

Contribution from the Equipe de Dynamique des Assemblages Membranaires, UMR CNRS/UHP 7565, Institut Nancéien de Chimie Moléculaire, Université Henri Poincaré, BP 239, 54506 Vandœuvre-lès-Nancy Cedex, France

Received October 24, 2002; E-mail: chipot@lctn.uhp-nancy.fr; collet@lctn.uhp-nancy.fr

Abstract: The unfolding of the last, C-terminal residue of $AcNH_2-(L\text{-}Leu)_{11}-NHMe$ in its α-helical form has been investigated by measuring the variation of free energy involved in the α_R to β conformational transition. These calculations were performed using large-scale molecular dynamics simulations in conjunction with the umbrella sampling method. For different temperatures ranging from 280 to 370 K, the free energy of activation was estimated. Concurrently, unfolding simulations of a homopolypeptide formed by twelve hydrophobic residues were carried out, employing a three-dimensional lattice model description of the peptide, with a temperature-dependent interaction potential. Using a Monte Carlo approach, the lowest free energy conformation, an analogue of a right-handed α-helix, was determined in the region where the peptide chain is well ordered. The free energy barrier separating this state from a distinct, compact conformation, analogue to a β-strand, was determined over a large enough range of temperatures. The results of these molecular dynamics and lattice model simulations are consistent and indicate that the kinetics of the unfolding of a hydrophobic peptide exhibits a non-Arrhenius behavior closely related to the temperature dependence of the hydrophobic effect. These results further illuminate the necessity to include a temperature dependence in potential energy functions designed for coarse-grained models of proteins.

Introduction

In essence, the sequence of amino acids of a protein contains all the information necessary to determine the unique, compact structure of the chain that is relevant under given physiological conditions.[1] Furthermore, this native structure is biologically active and is reached within very short times. In the past decades, much attention has been paid to this biological problem, fueled by a prolific literature on both the experimental and the theoretical fronts. Capturing the underlying mechanisms of protein folding has rapidly become one of the current challenges of modern, theoretical biophysics.[2−30]

In 1959, Kauzmann showed that the main force driving a protein toward its native structure is rooted in the hydrophobic effect.[31] On account of its fundamental importance for protein

(1) Anfinsen, C. B. Principles that govern the folding of protein chains. *Science* **1973**, *181*, 223−227.
(2) Taketomi, H.; Ueda, Y.; Gō, N. Studies on protein folding, unfolding and fluctuations by computer simulation. 1. The effect of specific amino Acid sequence represented by specific inter-unit interactions. *Int. J. Pept. Protein Res.* **1975**, *7*, 445−459.
(3) Chan, H. S.; Dill, K. A. Polymer principles in protein structure and stability. *Annu. Rev. Biophys. Biophys. Chem.* **1991**, *20*, 447−490.
(4) Daggett, V.; Levitt, M. Molecular dynamics simluations of helix denaturation. *J. Mol. Biol.* **1992**, *223*, 1121−1138.
(5) Karplus, M.; Shakhnovich, E. Theoretical studies of thermodynamics and dynamics. In *Protein Folding*; Creighton, T. E., Ed.; W. H. Freeman and Company: New York, 1992; pp 127−193.
(6) Bryngelson, J. D.; Onuchic, J. N.; Socci, N. D.; Wolynes, P. G. Funnels, pathways and the energy landscape of protein folding: A synthesis. *Proteins: Struct., Funct., Genet.* **1995**, *21*, 167−195.
(7) Dill, K. A.; Bromberg, S.; Yue, K.; Fiebig, K. M.; Yee, D. P.; Thomas, P. D.; Chan, H. S. Principles of protein folding − A perspective from simple exact models. *Protein Sci.* **1995**, *4*, 561−602.
(8) Karplus, M.; Săli, A. Theoretical studies of protein folding and unfolding. *Curr. Opin. Struct. Biol.* **1995**, *5*, 58−73.
(9) Wolynes, P. G.; Onuchic, J. N.; Thirumalai, D. Navigating the folding routes. *Science* **1995**, *267*, 1619−1620.
(10) Brooks, C. L., III. Helix-coil kinetics: Folding time scales for helical peptides from a sequential kinetic model. *J. Phys. Chem.* **1996**, *100*, 2546−2549.
(11) Young, W. S.; Brooks, C. L., III. A microscopic view of helix propagation: N and C-terminal helix growth in alanine helices. *J. Mol. Biol.* **1996**, *259*, 560−572.
(12) Thirumalai, D.; Woodson, S. A. Kinetics of folding of proteins and RNA. *Acc. Chem. Res.* **1996**, *29*, 433−439.
(13) Skolnick, J.; Galazka, W.; Skolnick, J. On the origin of the cooperativity of protein folding: Implications from model simulations. *Proteins: Struct., Funct., Genet.* **1996**, *26*, 271−287.
(14) Dill, K. A.; Chan, H. S. From Levinthal to pathways to funnels. *Nat. Struct. Biol.* **1997**, *4*, 10−19.
(15) Hao, M. H.; Scheraga, H. A. Characterization of foldable protein models: Thermodynamics, folding kinetics and force fields. *J. Chem. Phys.* **1997**, *107*, 8089−8102.
(16) Onuchic, J. N.; Luthey-Schulten, Z.; Wolynes, P. G. Theory of protein folding: The energy landscape perspective. *Annu. Rev. Phys. Chem.* **1997**, *48*, 545−600.
(17) Pande, V. S.; Grosberg, A. Y.; Tanaka, T. Statistical mechanics of simple models of protein folding and design. *Biophys. J.* **1997**, *73*, 3192−3210.
(18) Shakhnovich, E. Theoretical studies of protein-folding thermodynamics and kinetics. *Curr. Opin. Struct. Biol.* **1997**, *7*, 29−40.
(19) Lazaridis, T.; Karplus, M. "New view" of protein folding reconciled with the old through multiple unfolding simulations. *Science* **1997**, *278*, 1928−1931.
(20) Chan, H. S.; Dill, K. A. Protein folding in the landscape perspective: Chevron plots and non-Arrhenius kinetics. *Proteins: Struct., Funct., Genet.* **1998**, *30*, 2−33.
(21) Pande, V. S.; Grosberg, A. Y.; Tanaka, T.; Rokhsar, D. S. Pathways for protein folding: Is a new view needed? *Curr. Opin. Struct. Biol.* **1998**, *8*, 68−79.
(22) Hao, M. H.; Scheraga, H. A. Molecular mechanisms for cooperative folding of proteins. *J. Mol. Biol.* **1998**, *277*, 973−983.
(23) Dobson, C. M.; Săli, A.; Karplus, M. Protein folding: A perspective from theory and experiment. *Angew. Chem., Int. Ed.* **1998**, *37*, 868−893.

folding, the hydrophobic effect constitutes in its own right an equally active field of research.[32−44] Among others, it has rationalized chemical phenomena like the transfer of a nonpolar solute from the gas phase to an aqueous medium − a process accompanied by an increase of the free energy, which explains why the hydrophobic residues of a protein are removed from water in the core of the chain.[45−48] Whereas an accurate description of the solvent may not necessarily be crucial for modeling protein folding, its influence on the conformation of the chain should be taken into account as accurately as possible.[49−54]

Two significant theoretical approaches for tackling the protein folding problem have been used extensively in recent years. In the first one, an all-atom representation of both the protein and its surroundings and an empirically based potential energy function are employed to evaluate the interactions of all components of the system.[55−58] This class of models is often coupled to a molecular dynamics (MD) scheme to explore the rugged phase space of the solvated protein.[59] Ab initio folding by means of atomic-level MD simulations featuring both the protein and the aqueous environment remain limited to short peptides and small proteins, mostly because such a detailed description of the system is computationally prohibitive and does not allow biologically relevant time scales, viz typically $t >$ 100 ns, to be accessed in a routine fashion.[60−65]

An alternative approach consists of resorting to a coarse-grained model, in which each monomer of the chain is described by a bead located at the vertex of a two- or three-dimensional lattice.[2] The energy of a conformation is evaluated as the sum of pairwise interactions of monomers that are first neighbors on the lattice. Until recently, two main classes of coupling had been used widely. In the HP model,[66,67] a monomer is either hydrophobic (H) or polar (P). The coupling terms are chosen so that the hydrophobic monomers aggregate in the core of the

(24) Li, A.; Daggett, V. Molecular dynamics simulation of the unfolding of barnase: Characterization of the major intermediate. *J. Mol. Biol.* **1998**, *275*, 677−694.
(25) Dill, K. A. Polymer principles and protein folding. *Protein Sci.* **1999**, *8*, 1166−1180.
(26) Thirumalai, D.; Klimov, D. K. Deciphering the time scales and mechanisms of protein folding using minimal off-lattice models. *Curr. Opin. Struct. Biol.* **1999**, *9*, 197−207.
(27) Buchler, N. E. G.; Goldstein, R. A. Universal correlation between energy gap and foldability for the random energy model and lattice proteins. *J. Chem. Phys.* **1999**, *111*, 6599−6609.
(28) Zhou, Y.; Hall, C. K.; Karplus, M. The calorimetric criterion for a two-state process revisited. *Protein Sci.* **1999**, *8*, 1064−1074.
(29) Chan, H. S. Modeling protein density of states: Additive hydrophobic effects are insufficient for calorimetric two-state cooperativity. *Proteins: Struct., Funct., Genet.* **2000**, *40*, 543−571.
(30) Collet, O. Warm and cold denaturation in the phase diagram of a protein lattice model. *Europhys. Lett.* **2001**, *53*, 93−99.
(31) Kauzmann, W. Some factors in the interpretation of protein denaturation. *Adv. Protein Chem.* **1959**, *14*, 1−63.
(32) Ben-Naim, A. Statistical mechanics of water-like particles in two dimensions. Physical Model. Application of the Perkus−Yevick equation. *J. Chem. Phys.* **1970**, *54*, 3682−3695.
(33) Pratt, L. R.; Chandler, D. Theory of hydrophobic effect. *J. Chem. Phys.* **1977**, *67*, 3683−3704.
(34) Pohorille, A.; Pratt, L. Cavities in molecular liquids and the theory of hydrophobic solubilities. *J. Am. Chem. Soc.* **1990**, *112*, 5066−5074.
(35) Pratt, L. R.; Pohorille, A. Theory of hydrophobicity: Transient cavities in molecular liquids. *Proc. Natl. Acad. Sci. U.S.A.* **1992**, *89*, 2995−2999.
(36) Hummer, G.; Garde, S.; Garcıa, A.; Pohorille, A.; Pratt, L. An information theory model of hydrophobic interactions. *Proc. Natl. Acad. Sci. U.S.A.* **1996**, *93*, 8951−8955.
(37) Lee, B.; Graziano, G. A Two-state model of hydrophobic hydration that produces compensating enthalpy and entropy changes. *J. Am. Chem. Soc.* **1996**, *118*, 5163−5168.
(38) Hummer, G.; Garde, S.; Garcia, A. E.; Paulaitis, M. E.; Pratt, L. R. Hydrophobic effects on a molecular scale. *J. Phys. Chem. B* **1998**, *102*, 10469−10472.
(39) Gomez, M. A.; Pratt, L. R.; Hummer, G.; Garde, S. Molecular realism in default models for information theories of hydrophobic effects. *J. Phys. Chem. B* **1999**, *103*, 3520−3523.
(40) Silverstein, K. A. T.; Haymet, A. D. J.; Dill, K. A. Molecular model of hydrophobic solvation. *J. Chem. Phys.* **1999**, *111*, 8000−8009. (The energy spectrum used in the present work are derived from the results shown in Figure 3.)
(41) Pratt, L. R. Molecular theory of hydrophobic effects: She is too mean to have her name repeated. *Annu. Rev. Phys. Chem.* **2002**, *53*, 409−436.
(42) Pratt, L. R.; Pohorille, A. Hydrophobic effects and modeling of biophysical aqueous solution interfaces. *Chem. Rev.* **2002**, *102*, 2671−2692.
(43) Shimizu, S.; Chan, H. S. Anti-cooperativity and cooperativity in hydrophobic interactions: Three-body free energy landscapes and comparison with implicit-solvent potential functions for proteins. *Proteins: Struct., Funct., Genet.* **2002**, *48*, 15−30.
(44) Czaplewski, C.; Ripoll, D. R.; Liwo, A.; Rodziewicz-Motowidlo, S.; Wawak, J.; Scheraga, H. A. Can cooperativity in hydrophobic association be reproduced correctly by implicit solvation models? *Int. J. Quantum Chem.* **2002**, *88*, 41−45.
(45) Hodes, Z. I.; Némethy, G.; Scheraga, H. A. Model for the conformational analysis of hydrated peptides. Effect of hydration on the conformational stability of the terminally blocked residues of the 20 naturally occurring amino acids. *Biopolymers* **1979**, *18*, 1565−1610.
(46) Kang, Y. K.; Néméthy, G.; Scheraga, H. A. Free energies of hydration of solute molecules. Improvement of the hydration shell model by exact computations of overlapping volumes. *J. Phys. Chem.* **1987**, *91*, 4105−4109.
(47) Garde, S.; Hummer, G.; Garcia, A. E.; Paulaitis, M. E.; Pratt, L. R. Origin of entropy convergence in hydrophobic hydration and protein folding. *Phys. Rev. Lett.* **1996**, *77*, 4966−4968.
(48) Sorenson, J. M.; Hura, G.; Soper, A. K.; Pertsemlidis, A.; Head-Gordon, T. Determining the role of hydration forces in protein folding. *J. Phys. Chem. B* **1999**, *103*, 5413−5426.
(49) Gilson, M. K.; Rashin, A.; Fine, R.; Honig, B. H. On the calculation of electrostatic interactions in proteins. *J. Mol. Biol.* **1985**, *184*, 503−516.
(50) Collet, O.; Premilat, S.; Maigret, B.; Scheraga, H. A. Comparison of explicit and implicit treatments of solvation: Application to angiotensin II. *Biopolymers* **1997**, *42*, 363−371.
(51) Roux, B.; Simonson, T. Implicit solvent models. *Biophys. Chem.* **1999**, *78*, 1−20.
(52) Lazaridis, T.; Karplus, M. Discrimination of the native from misfolded protein models with an energy function including implicit solvation. *J. Mol. Biol.* **1999**, *288*, 477−487.
(53) Ferrara, P.; Apostolakis, J.; Caflisch, A. Evaluation of a fast implicit solvent model for molecular dynamics simulations. *Proteins: Struct., Funct.ion, Genet.* **2002**, *46*, 24−33.
(54) Gsponer, J.; Caflisch, A. Molecular dynamics simulations of protein folding from the transition state. *Proc. Natl. Acad. Sci. U.S.A.* **2002**, *99*, 6719−6724.
(55) Ripoll, D. R.; Scheraga, H. A. ECEPP: Empirical conformational energy program for peptides. In *Encyclopedia of Computational Chemistry*; Schleyer, P. v. R., Allinger, N. L., Clark, T., Gasteiger, J., Kollman, P. A., Schaefer, H. F., III., Schreiner, P. R., Eds.: Wiley and Sons: Chichester, U.K., 1998; Vol. 2, pp 813−815.
(56) MacKerell, A. D., Jr.; Bashford, D.; Bellott, M.; Dunbrack, R. L., Jr.; Evanseck, J. D.; Field, M. J.; Fischer, S.; Gao, J.; Guo, H.; Ha, S.; Joseph-McCarthy, D.; Kuchnir, L.; Kuczera, K.; Lau, F. T. K.; Mattos, C.; Michnick, S.; Ngo, T.; Nguyen, D. T.; Prodhom, B.; Reiher, W. E., III.; Roux, B.; Schlenkrich, M.; Smith, J. C.; Stote, R.; Straub, J.; Watanabe, M.; Wiórkiewicz-Kuczera, J.; Yin, D.; Karplus, M. All-atom empirical potential for molecular modeling and dynamics studies of proteins. *J. Phys. Chem. B* **1998**, *102*, 3586−3616.
(57) Cornell, W. D.; Cieplak, P.; Bayly, C. I.; Gould, I. R.; Merz, K. M., Jr.; Ferguson, D. M.; Spellmeyer, D. C.; Fox, T.; Caldwell, J. C.; Kollman, P. A. A second generation force field for the simulation of proteins, nucleic acids, and organic molecules. *J. Am. Chem. Soc.* **1995**, *117*, 5179−5197.
(58) Wang, J.; Cieplak, P.; Kollman P. A. How well does a restrained electrostatic potential (RESP) model perform incalculating conformational energies of organic and biological molecules? *J. Comput. Chem.* **2000**, *21*, 1049−1074.
(59) Karplus, M.; Petsko, G. A. Molecular dynamics simulations in biology. *Nature* **1990**, *347*, 631−639.
(60) Demchuk, E.; Bashford, D.; Case, D. A. Dynamics of a type IV turn in a linear peptide in aqueous solution. *Folding Des.* **1997**, *2*, 35−46.
(61) Chipot, C.; Pohorille, A. Folding and translocation of the undecamer of poly-L-leucine across the water-hexane interface. A multi-nanosecond molecular dynamics study. *J. Am. Chem. Soc.* **1998**, *120*, 11912−11924.
(62) Daura, X.; Jaun, B.; Seebach, D.; van Gunsteren, W. F.; Mark, A. E. Reversible peptide folding in solution by molecular dynamics simulation. *J. Mol. Biol.* **1998**, *280*, 925−932.
(63) Duan, Y.; Kollman, P. A. Pathways to a protein folding intermediate observed in a 1-microsecond simulation in aqueous solution. *Science* **1998**, *282*, 740−744.
(64) Chipot, C.; Maigret, B.; Pohorille, A. Early events in the folding of an amphipathic peptide. A multi-nanosecond molecular dynamics study. *Proteins: Struct., Funct., Genet.* **1999**, *36*, 383−399.
(65) Daggett, V. Long time-scale simulations. *Curr. Opin. Struct. Biol.* **2000**, *10*, 160−164.
(66) Lau, K. F.; Dill, K. A. A lattice statistical mechanics model of the conformational and sequence spaces of proteins. *Macromolecules* **1989**, *22*, 3986−3997.
(67) Chan, H. S.; Dill, K. A. Energy landscapes and the collapse dynamics of homopolymers. *J. Chem. Phys.* **1993**, *99*, 2116−2127.

chain. In the so-called random energy model (REM),[68] on the other hand, the coupling terms are taken randomly from a Gaussian distribution, so that the ground state of the energy spectrum characterizing the chain is a unique, compact conformation.[18,69,70] Although the HP and the REM models have been shown to mimic rather well the thermodynamic properties of a protein at a given temperature, it has been suggested, on account of the very strong influence of the temperature on the hydrophobic effect,[41,42] that the coupling terms utilized in lattice models should be temperature dependent.[30,71−74] Interestingly enough, the temperature dependence of hydrophobic interactions was first introduced by Dill and Chan to describe non-Arrhenius kinetics in protein folding simulations.[20,75]

We have proposed recently that the free energy of solvation of the monomers and that of the bulk solvent could be incorporated in the model in terms of effective, pairwise interactions of monomers, without increasing the complexity of the approach nor the computational effort.[30] Based on a study of the hydrophobic effect with a minimalist model of water,[32,40] a temperature dependence of the coupling terms in the REM has been introduced. The latter allows the computation of the phase diagram of a protein, which exhibits domains characteristic of both warm and cold denaturations,[76,77] in good agreement with experimental results.[78,79]

The main thrust of the present contribution is to confront simulations of the folding/unfolding of a hydrophobic homopolypeptide, using MD in association with an all-atom description of the system and lattice models with temperature-dependent potentials. The reaction pathway connecting the α-helix and the β-strand conformations of the last, C-terminal residue of the terminally blocked $AcNH_2-(L\text{-}Leu)_{11}-NHMe$ has been computed by MD, over a range of temperatures. A similar investigation of analogues of the α-helix and the β-strand has been carried out using a three-dimensional lattice model. The resulting activation free energies were determined as a function of the temperature, employing the two alternative methods which agree very well on a qualitative level. Although the work described herein is not a kinetics study per se, the kinetics behavior of the system can be inferred based on the determined equilibrium thermodynamics properties, relating the evolution of the folding/unfolding rate with temperature to the free energy of activation in the framework of the activated complex theory. The results of this synergistic work targeted at the comparison of MD and lattice model simulations strongly support the temperature dependence of the coupling terms used in the lattice models.

Methods

The partition function of the system formed by the hydrophobic homopolypeptide in conformations m, solvated by water molecules organized in configurations m', is given by

$$Z(T) = \sum_{m}\sum_{m'} \exp\left(-\frac{\mathcal{O}_{\text{intra}}^{(m)} + \mathcal{O}_{\text{hydr}}^{(mm')}}{k_B T}\right) \quad (1)$$

where $\mathcal{O}_{\text{intra}}^{(m)}$ is the intrachain energy, which is a sole function of the peptide conformation. $\mathcal{O}_{\text{hydr}}^{(mm')}$ is the hydration contribution, which includes peptide-solvent and solvent-solvent interactions. T is the temperature, and k_B is the Boltzmann constant. It is worth noting that in eq 1, the ensemble of configurations m' accessible to the solvent depend on the conformation, m, of the peptide chain. The temperature-dependent weight of conformation m can be expressed as

$$\omega_m(T) = \sum_{m'} \exp\left(-\frac{\mathcal{O}_{\text{intra}}^{(m)} + \mathcal{O}_{\text{hydr}}^{(mm')}}{k_B T}\right) \quad (2)$$

In the MD simulations reported herein, an "all-atom" representation of both the peptide and its aqueous environment was adopted, and the summation over configurations of the solvent for a given conformation of the peptide chain is explicit. In sharp contrast, the three-dimensional lattice model simulations presented in this work rely on a mean field description of the solvent, as will be detailed in the following.

2.1. Molecular Dynamics Free Energy Calculations. 2.1.1. Description of the System and Simulation Protocol. The system consisted of an undecamer of L-leucine, blocked at its N- and C-termini by an Ac− and an −NHMe group, respectively, and immersed in a cell of 1657 water molecules. In all MD simulations, the initial structure of the peptide was an α_R-helix. The dimensions of the simulation box were $37.1 \times 37.1 \times 37.1$ Å^3. Periodic boundary conditions were applied in all three directions of space.[80] Water molecules were described using the TIP4P model.[81] Bond stretching, valence angle deformation, torsional, and nonbonded parameters of the undecamer of L-leucine were extracted from the all-atom AMBER force field of Wang et al.[58]

All MD simulations were performed in the canonical (N, V, T) ensemble,[80] using the COSMOS program.[82] The SHAKE algorithm[83] was employed to constrain the length of the chemical bonds between hydrogen and heavy atoms. The equations of motion were integrated using the velocity Verlet algorithm with a time-step of 2.0 fs.[84] The temperature of the system was maintained at the desired value by means of the extended system, Nosé−Hoover algorithm.[85,86] To examine the influence of the temperature on the activation free energy involved in

(68) Derrida, B. Random-energy model: An exactly solvable model of disordered systems. *Phys. Rev. E* **1981**, *24*, 2613−2626.
(69) Shakhnovich, E. I.; Gutin, A. M. Formation of unique structure in polypeptide chains: Theoretical investigation with the aid of a replica approach. *Biophys. Chem.* **1989**, *34*, 187−199.
(70) Shakhnovich, E. I.; Gutin, A. M. Implications of thermodynamics of protein folding for evolution of primary sequences. *Nature* **1990**, *346*, 773−775.
(71) Premilat, S.; Collet, O. Hydration effects in a lattice model of protein folding. *Europhys. Lett.* **1997**, *39*, 575−580.
(72) Hansen, A.; Jensen, M. H.; Sneppen, K.; Zocchi, G. Statistical mechanics of warm and cold unfolding in proteins. *Eur. Phys. J. B* **1998**, *6*, 157−161.
(73) De Los Rios, P.; Caldarelli, G. Putting proteins back into water. *Phys. Rev. E* **2000**, *62*, 8449−8452.
(74) Shimizu, S.; Chan, H. S. Temperature dependence of hydrophobic interactions: A mean force perspective, effects of water density, and nonadditivity of thermodynamics signature. *J. Am. Chem. Soc.* **2000**, *113*, 4683−4700.
(75) Chan, H. S. Modeling protein folding by Monte Carlo dynamics: Chevron plots. Chevron roll-overs and non-Arrhenius kinetics. In *Monte Carlo Approach to Biopolymer and Protein Folding*; Grassberger, P., Barkema, G. T., Nadler, W., Eds.; World Scientific: Singapore, 1998; pp 29−44.
(76) Nishi, I.; Kataoka, N.; Tokunaga, F.; Goto, Y. Cold denaturation of the molten globule states of apomyoglobin and a profile for protein folding. *Biochemistry* **1994**, *33*, 4903−4909.
(77) Nölting, B. *Protein Folding Kinetics*; Springer-Verlag: Berlin, 1999.
(78) Privalov, P. L.; Makhatadze, G. I. Heat capacity and conformation of proteins in the denatured state. *J. Mol. Biol.* **1989**, *205*, 737−750.
(79) Privalov, P. L. Cold denaturation of proteins. *Crit. Rev. Biochem. Mol. Biol.* **1990**, *25*, 281−305.
(80) Allen, M. P.; Tildesley, D. J. *Computer Simulation of Liquids*; Clarendon Press: Oxford, 1987.
(81) Jorgensen, W. L.; Chandrasekhar, J.; Madura, J. D.; Impey, R. W.; Klein, M. L. Comparison of simple potential functions for simulating liquid water. *J. Chem. Phys.* **1983**, *79*, 926−935.
(82) Owenson, B.; Wilson, M. A.; New, M. H.; Couturier, R.; Rozanska, M. A.; Chipot, C.; Pohorille, A. *COSMOS* − A software package for COmputer Simulations of MOlecular Systems. NASA − Ames Research Center: Moffett Field, CA 94035-1000, 2001.
(83) Ryckaert, J.; Ciccotti, G.; Berendsen, H. J. C. Numerical integration of the Cartesian equations of motion for a system with constraints: Molecular dynamics of *n*-alkanes. *J. Comput. Phys.* **1977**, *23*, 327−341.
(84) Frenkel, D.; Smit, B. *Understanding molecular simulations: From algorithms to applications*; Academic Press: San Diego, CA, 1996.
(85) Nosé, S. A molecular dynamics method for simulations in the canonical ensemble. *Mol. Phys.* **1984**, *52*, 255−268.
(86) Hoover, W. G. Canonical dynamics: Equilibrium phase-space distributions. *Phys. Rev.* **1985**, *A31*, 1695−1697.

the unfolding of the last C-terminal residue of $AcNH_2-(L\text{-}Leu)_{11}-NHMe$, the system was simulated at six distinct temperatures, viz 280, 300, 320, 340, 360, and 370 K. To warrant that the volume of the cell corresponds to the correct density at these temperatures, a preliminary equilibration was carried out in the isobaric−isothemal, (N, P, T) ensemble, employing a hybrid Monte Carlo (HMC) approach.[87,88] For each temperature, the system was sampled over 1750 HMC passes of 200 MD steps, until the volume of the cell reached a stable plateau.

Water−water nonbonded interactions were truncated smoothly between 7.5 and 8.0 Å.[89] A smooth cutoff ranging between 9.5 and 10.0 Å was adopted to truncate the water−peptide interactions. No truncation was applied to peptide−peptide nonbonded interactions. Using this protocol, the observed root-mean-square deviation (RMSD) in the total energy, that is, system plus thermostat, was 5.3 kcal/mol over 100 ps of MD, corresponding to a drift of less than 0.2%.

2.1.2. Free Energy Calculations. The main thrust of this contribution is to investigate the influence of the temperature on the thermodynamic and the kinetic properties of the unfolding of a short, hydrophobic peptide. The free energy for converting the last C-terminal residue from an α-helical to a β-strand conformation was determined at six distinct temperatures, viz 280, 300, 320, 340, 360, and 370 K, using the so-called "umbrella sampling" (US) method.[90] The reaction coordinate was the last ψ angle of the homopolypeptide,[11] all other torsional angles being restrained softly in a range of values characteristic of an α_R-helix, that is, $-77 \le \phi_i \le -37°, \forall i$ and $-67 \le \psi_i \le -27°, \forall i \neq 11$.

For each temperature, the complete reaction pathway that connects the α-helical state to the β-strand was decomposed into five overlapping "windows",[91] in which the reaction coordinate, ψ, was restrained by means of a quadratic biasing potential, $\mathcal{U}_{bias}(\psi)$. In addition, to guarantee that all values accessible to ψ in the window of interest be sampled uniformly, an additional linear external potential, $\mathcal{U}_{bias}(\psi)$, was included in the MD simulations, so that the free energy writes

$$A(\psi) = -k_B T \ln \mathcal{P}_{bias}(\psi) + \mathcal{U}_{bias}(\psi) + \mathcal{U}'_{bias}(\psi) + A_0(\psi) \quad (3)$$

where $A_0(\psi)$ is a constant term. The full free energy profiles were obtained in a self-consistent fashion, employing the weighted histogram analysis method (WHAM).[92] The force constant used to restrain sampling to a window of interest, by means of a biasing potential, $\mathcal{U}_{bias}(\psi)$, is equal to 0.1 kcal/mol deg^2, irrespective of the window. In contrast, the force constant chosen for the linear potential, $\mathcal{U}'_{bias}(\psi)$, inherently depends on the shape of the free energy profile for a given window and the temperature at which the latter is sampled. Here, the force constants utilized ranged between ca. −0.06 and +0.06 kcal/mol deg, with $-90 \le \psi_{11} \le 170°$.

The total simulation times required to reach converged free energies are reported in Table 1. The significant length of these US simulations can be ascribed to the necessity to sample appropriately those degrees of freedom orthogonal to the reaction coordinate,[93,94] ψ. Convergence of $\mathcal{P}_{bias}(\psi)$ is limited by self-diffusion within the "window" of interest, which is greatly impeded at low temperatures. As a result, the total simulation time progressively increases as the temperature decreases. At 280 K, sampling is quasi nonergodic, which is illustrated by the difficulty to explore efficiently the high free energy region separating the α-helix from the β-strand conformations.

Table 1. Simulation Times for the Umbrella Sampling Free Energy Calculations of the α-Helix to β-Strand Conformational Transition in $AcNH_2-(L\text{-}Leu)_{11}-NHMe$

	time per window (ns)					
temp (K)	1[a]	2[a]	3[a]	4[a]	5[a]	total time (ns)
280.0	12.0	16.0	24.0	12.0	12.0	76.0
300.0	2.5	2.5	10.5	10.5	4.0	30.0
320.0	1.0	3.0	10.0	3.0	4.0	21.0
340.0	1.5	2.5	9.5	2.0	7.0	22.5
360.0	1.0	1.5	4.0	4.0	4.0	14.5
370.0	1.0	1.5	4.0	4.0	3.5	14.0

[a] (1) $-90.00 \le \psi \le 0.00$; (2) $-20.00 \le \psi \le 60.00$; (3) $40.00 \le \psi \le 100.00$; (4) $80.00 \le \psi \le 120.00$; (5) $100.00 \le \psi \le 170.00$.

The error affecting the final free energy differences stems from two distinct contributions. The first is the statistical error that reflects sampling inaccuracies for each value of ψ along the reaction coordinate. This contribution can be inferred by dividing the simulation of a given window into batches, from which a root-mean-square deviation (RMSD) is computed. Here, the complete sampling per window was broken down into subruns of 20 ps. The second contribution is a systematic error arising from differences in the curvature of consecutive free energy profiles in their overlapping region. This term was estimated from a piecewise matching of the free energy profiles in adjacent windows, by minimizing the RMSD between their respective curvatures. It will be assumed that the statistical and the systematic errors are uncorrelated and can, thus, be estimated independently.

2.2. Lattice Model Simulations. 2.2.1. Mean Field Description of the Environment. In contrast with the all-atom representation adopted in the previous MD free energy calculations, the homopolypeptide now consists of a linear chain of twelve beads located on a three-dimensional lattice. The originality of the lattice model employed herein lies in the inclusion of the surroundings through a mean field description of the aqueous environment.[30] Each vertex of the three-dimensional lattice that is not occupied by a nonpolar monomer of the peptide chain constitutes a site of hydration, analogous in spirit to an ensemble of water molecules. Because the ensemble of configurations accessible to the solvent inherently depends on the conformation of the homopolypeptide, the hydration free energy of the latter can be expressed as[50,71]

$$A^{(m)}_{hydr}(T) = -T \ln \sum_{m'} \exp\left(-\frac{\mathcal{O}^{(mm')}_{hydr}}{T}\right) \quad (4)$$

Here, the energy units are chosen, so that the Boltzmann constant, k_B, equals 1. The partition function in eq 1 can then be restated in the simpler form:

$$Z(T) = \sum_m \exp\left(-\frac{A^{(m)}_{total}(T)}{T}\right) \quad (5)$$

where the total free energy of the peptide chain in its conformation m is

$$A^{(m)}_{total}(T) = \mathcal{O}^{(m)}_{intra} + A^{(m)}_{hydr}(T) \quad (6)$$

This equation indicates that the temperature dependence of the potentials appears in the formalism via its solvent contribution. From the

(87) Duane, S.; Kennedy, A. D.; Pendleton, B. J.; Roweth, D. Hybrid Monte Carlo. *Phys. Lett. B* **1987**, *195*, 216−222.
(88) Mehlig, B.; Herrmann, D. W.; Forrest, B. M. Hybrid Monte Carlo method for condensed-matter systems. *Phys. Rev. B* **1992**, *45*, 679−685.
(89) Andrea, T. A.; Swope, W. C.; Andersen, H. C. The role of long-ranged forces in determining the structure and properties of liquid water. *J. Chem. Phys.* **1983**, *79*, 4576−4584.
(90) Torrie, G. M.; Valleau, J. P. Nonphysical sampling distributions in Monte Carlo free energy estimation: Umbrella sampling. *J. Comput. Phys.* **1977**, *23*, 187−199.
(91) Valleau, J. P.; Card, D. N. Monte Carlo estimation of the free energy by multistage sampling. *J. Chem. Phys.* **1972**, *57*, 5457−5462.
(92) Kumar, S.; Bouzida, D.; Swendsen, R. H.; Kollman, P. A.; Rosenberg, J. M. The weighted histogram analysis method for free energy calculations on biomolecules. I. The method. *J. Comput. Chem.* **1992**, *13*, 1011−1021.
(93) Mark, A. E. Free Energy Perturbation Calculations. In *Encyclopedia of Computational Chemistry*; Schleyer, P. v. R., Allinger, N. L., Clark, T., Gasteiger, J., Kollman, P. A., Schaefer, H. F., III., Schreiner, P. R., Eds.; Wiley and Sons: Chichester, U.K., 1998; Vol. 2, pp 1070−1083.
(94) Chipot, C.; Pearlman, D. A. Free energy calculations. The long and winding gilded road. *Mol. Simul.* **2002**, *28*, 1−12.

above, it becomes clear that the potential of mean force introduced in the formalism to account for the environment of the peptide is necessarily the conformational free energy of the homopolypeptide that incorporates the entropic contribution due to the solvent and not a mere temperature-independent conformational energy, as is often used in lattice models. Equation 6 is restated as a sum of effective, pairwise interactions, $A^{(m)}_{\text{pairwise}}(T)$, and a specific, many-body potential that models helix formation, $\mathcal{O}^{(m)}_{\text{helix}}$:

$$A^{(m)}_{\text{total}}(T) = A^{(m)}_{\text{pairwise}}(T) + \mathcal{O}^{(m)}_{\text{helix}} \tag{7}$$

2.2.2. Effective Pairwise Interactions. The additive pairwise contribution to the free energy of any given conformation *m* is determined as a function of the temperature and of a parameter, B_s, that characterizes the quality of the solvent; viz $B_s < 0$ corresponds to a poor solvent, conducive to a collapse of the chain, whereas $B_s > 0$ denotes a good solvent, likely to dissolve the homopolypeptide, thereby impeding folding. Choosing conventionally the extended structures, that feature no contact between monomers, as the reference state, we are able to write the free energy difference between conformation *m* and any extended conformer of the peptide chain as:

$$\Delta A^{(m)}_{\text{pairwise}}(B_s;T) = \sum_{i}^{12}\sum_{j>i}^{12} B^{\text{eff}}(B_s;T)\,\Delta^{(m)}_{ij} = n^{(m)}_{\text{intra}} B^{\text{eff}}(B_s;T) \tag{8}$$

Here, $\Delta^{(m)}_{ij} = 1$ if residues *i* and *j* are first neighbors on the lattice and 0 otherwise, and $n^{(m)}_{\text{intra}} = \sum_i^{12}\sum_{j>i}^{12}\Delta^{(m)}_{ij}$ is the number of intrachain contacts. $B^{\text{eff}}(B_s;T)$ denotes the effective coupling between two monomers. In contrast with the heteropolymer model, the effective coupling, $B^{\text{eff}}(B_s;T)$, is independent of *i* and *j*, owing to the identical hydrophobic nature of the residues forming the homopolypeptide. The coupling term then writes as

$$B^{\text{eff}}(B_s;T) = B_H - 2f_H(T) + f_s(B_s;T) \tag{9}$$

where $B_H = -1$ represents the contribution of intrachain interactions.[66,70] The creation of such an interaction implies the deletion of two peptide−solvent bonds, hence the factor 2 in eq 9. The temperature-dependent peptide−solvent contributions that vanish when residues *i* and *j* associate can be expressed simply as

$$f_H(T) = -T \ln \sum_{j=1}^{N_s} \exp(-B_j/T) \tag{10}$$

B_j is the interaction energy of a hydrophobic monomer with a neighboring site of hydration, that is, an unoccupied vertex, that characterizes configuration *j* of the solvent among the N_s possible configurational states that the latter can adopt; here, $N_s = 10^5$. Values of B_j are taken from a Gaussian distribution that encompasses the N_s states of the solvent around residue *i*.[40] This distribution is centered at 0, and its standard deviation is equal to 1.

Contact of any pair of monomers results in an interaction of two sites of hydration, described by free energy contribution $f_s(B_s;T)$:

$$f_s(B_s;T) = B_s - T \ln N_s \tag{11}$$

B_s corresponds to the mean energy arising from the interaction of two sets of water molecules located on contiguous vertexes of the lattice. The energy spectrum of the neat solvent, narrower than that of the solvent interacting with a hydrophobic monomer, features a single N_s-fold degenerated level of energy, B_s, characterizing the solvation properties of the environment.[40]

2.2.3. Potential of Helix Formation. Because the probabilities to form a right-handed and a left-handed α-helix, starting from an extended conformer of the homopolypetide, are equal, the last term of eq 7 constitutes a bias to promote folding into the second conformational state, at the expense of the first:[95,96]

$$\mathcal{O}^{(m)}_{\text{helix}} = n^{(m)}_{\alpha_R}\epsilon_{\alpha_R} + n^{(m)}_{\alpha_L}\epsilon_{\alpha_L} \text{ with } \epsilon_{\alpha_R} < 0 < \epsilon_{\alpha_L} \tag{12}$$

$\epsilon_{\alpha R}$ and $\epsilon_{\alpha L}$ stand for the energy of one helical contact in a right-handed and a left-handed α-helix, respectively, and $n^{(m)}_{\alpha_R}$ and $n^{(m)}_{\alpha_L}$ are their respective population for conformation *m*. Here, $\epsilon_{\alpha_R} = -2$ and $\epsilon_{\alpha_L} = 5$, guaranteeing that the left-handed conformation will be seldom encountered.

2.2.4. Heat Capacity of the System. The heat capacity of the system is given by

$$C(B_s;T) = \frac{\langle \mathcal{O}_{\text{total}}{}^2\rangle - \langle \mathcal{O}_{\text{total}}\rangle^2}{T^2} \tag{13}$$

where $\langle\cdots\rangle$ denotes a thermal average over chain conformations. By analogy with eqs 7−9, the total energy of the system, wherein the chain is in conformation *m*, is given by

$$\mathcal{O}^{(m)}_{\text{total}}(B_s, T) = \mathcal{O}^{(m)}_{\text{pairwise}}(B_s, T) + \mathcal{O}^{(m)}_{\text{helix}} \tag{14}$$

$\mathcal{O}^{(m)}_{\text{pairwise}}(B_s, T)$ corresponds to the mean energy, sum of all pairwise interactions:

$$\mathcal{O}^{(m)}_{\text{pairwise}}(B_s, T) = n^{(m)}_{\text{intra}} D^{\text{eff}}(B_s, T) \tag{15}$$

where the effective mean energy, $D^{\text{eff}}(B_s, T)$, is given by

$$D^{\text{eff}}(B_s, T) = B_H - 2\overline{B_{HS}}(T) + B_s \tag{16}$$

The mean energy of solvation, $\overline{B_{HS}}(T)$, is simply the average over solvent configurations of the energy of solvation, B_j:

$$\overline{B_{HS}}(T) = \sum_{j=1}^{N_s} B_j \exp\left(\frac{f_H(T) - B_j}{T}\right) \tag{17}$$

3. Results and Discussion

3.1. Molecular Dynamics Free Energy Calculations. The free energy profiles delineating the unfolding of $AcNH_2$−(L-Leu)$_{11}$−NHMe at its C-terminus are shown in Figure 1. From the onset, it can be seen that the α-helix and the *β*-strand are two local minima of the conformational free energy landscape, and the α-helical state corresponds to a lower free energy than that of the *β*-strand, irrespective of the temperature. As indicated in Table 2, the free energy barrier involved in the transition from the α_R to the *β* conformation is substantial, ranging from 5.9 to 7.0 kcal/mol for $\Delta A_{\alpha_R\to\ddagger}$ and 0.7 to 2.2 kcal/mol for $\Delta A_{\beta\to\ddagger}$. The three key conformations, that is, the α-helix, the transition state, ‡, and the *β*-strand, can be characterized by their solvent accessible surface area (SASA). The latter has been estimated using the SERF program[97] with the Shrake and Rupley algorithm[98] and a probe of 1.4 Å. Limited to the C-terminal residue of the homopolypeptide, the SASA was found to be equal to 134 ± 2, 149 ± 7, and 117 ± 13 Å^2 for the α-helix, the transition state, and the *β*-strand, respectively. From these

(95) Kaya, H.; Chan, H. S. Energetic components of cooperative protein folding. *Phys. Rev. Lett.* **2000**, *85*, 4823−4826.
(96) Kaya, H.; Chan, H. S. Towards a consistent modeling of protein thermodynamic and kinetic cooperativity: How applicable is the transition state picture to folding and unfolding? *J. Mol. Biol.* **2002**, *315*, 899−909.
(97) Flower, D. R. SERF: A program for accessible surface area calculations. *J. Mol. Graphics Modell.* **1997**, *15*, 238−244.
(98) Shrake, A.; Rupley, J. A. Environment and exposure to solvent of protein atoms. Lysozyme and insulin. *J. Mol. Biol.* **1973**, *79*, 351−371.

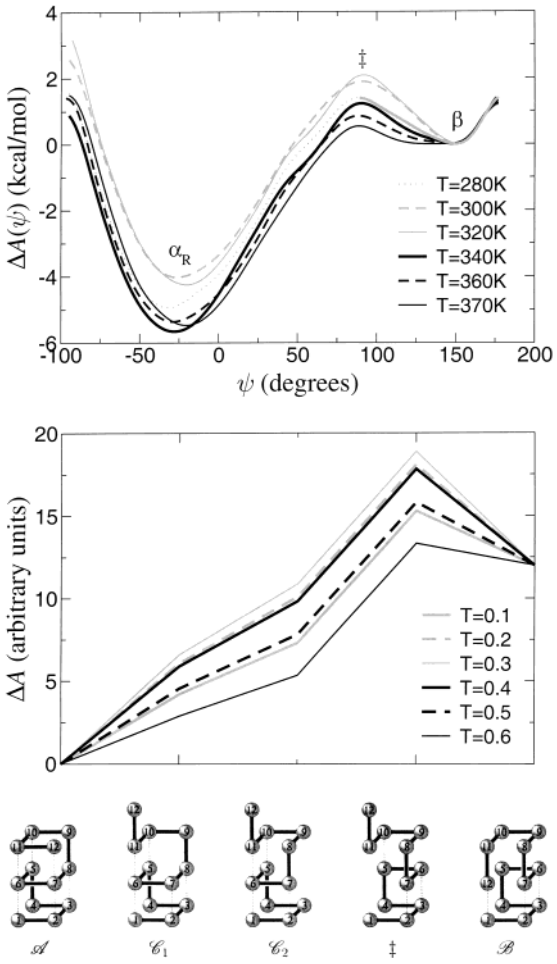

Figure 1. Free energy profiles characterizing the unfolding of a nonpolar homopolypeptide at different temperatures, using classical MD (upper) and lattice model (lower) simulations. In MD free energy calculations, the reaction coordinate is the ψ torsional angle of the C-terminus residue of $AcNH_2-(L\text{-}Leu)_{11}-NHMe$. The dotted line for the α-helix to ‡ transition at 280 K denotes a simulation not yet converged after 76 ns of MD sampling. In lattice model simulations, the transition from $\mathscr{A}$ to $\mathscr{B}$, the analogues of an α-helix and a β-strand, respectively, follows the reaction path depicted at the bottom of the figure.

Table 2. Free Energy Changes Involved in the α-Helix to β-Strand Conformational Transition of $AcNH_2-(L\text{-}Leu)_{11}-NHMe$

temp (K)	$\Delta A_{\alpha\to\beta}$ (kcal/mol)	$\Delta A_{\alpha\to\ddagger}$ (kcal/mol)	$\Delta A_{\beta\to\ddagger}$ (kcal/mol)
280.0	not converged	not converged	1.5 ± 0.2
300.0	4.0 ± 0.3	6.0 ± 0.3	2.0 ± 0.3
320.0	4.3 ± 0.2	6.5 ± 0.2	2.2 ± 0.2
340.0	5.7 ± 0.2	7.0 ± 0.2	1.3 ± 0.2
360.0	5.4 ± 0.1	6.4 ± 0.1	1.0 ± 0.1
370.0	5.2 ± 0.1	5.9 ± 0.1	0.7 ± 0.1

values, it is apparent that the exposure of the C-terminal to the aqueous environment is the largest for the transition state.

As mentioned previously, the quasi nonergodic behavior of the system at low temperatures impedes the efficient sampling of the region near the transition state. Considering the shape of the free energy profiles generated at different temperatures, we believe it is unlikely that the poor convergence witnessed at 280 K would be the result of an inappropriate choice of $\mathscr{U}'_{\text{bias}}(\psi)$, the external biasing potential that guarantees a uniform probability of encountering all possible values of the reaction coordinate within a given "window". In this sense, algorithms

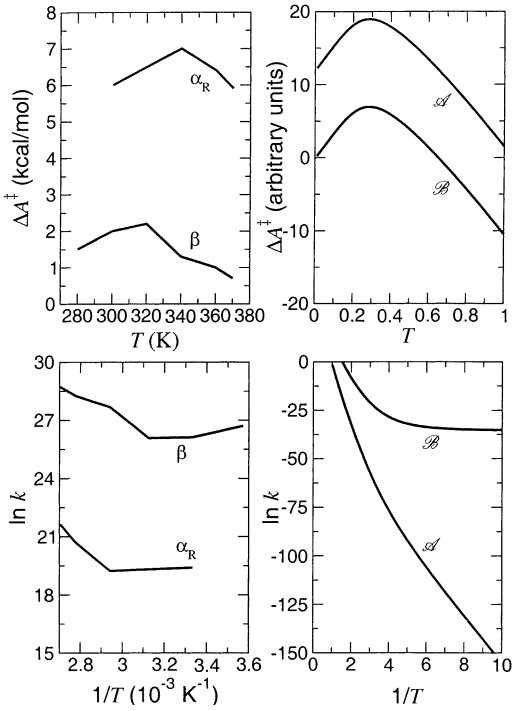

Figure 2. Activation free energies for the α-helix to ‡ and β-strand to ‡ transitions of $AcNH_2-(L\text{-}Leu)_{11}-NHMe$ (top left) and the $\mathscr{A}$ to ‡ and $\mathscr{B}$ to ‡ transitions of a 12-residue lattice model (top right), as a function of the temperature. Arrhenius plots for the same transitions in $AcNH_2-(L\text{-}Leu)_{11}-NHMe$ (bottom left) and in the 12-residue lattice model (bottom right), inferred from the activated complex theory, viz $\ln k = \ln k_B T/h - \Delta A^{\ddagger}/k_B T$, where h is the Planck constant, and the corresponding equilibrium activation free energies.

that do not require an a priori guess of the biasing potentials, like the recent adaptive force bias (AFB) method[99,100] or the multidimensional adaptive US,[101] may not necessarily perform better than the classical US approach. Despite extensive sampling, attaining altogether 76 ns, we believe convergence of the free energy profile at 280 K remains doubtful. In particular, the difficulty to match "windows" 2 and 3 calls into question the convergence of these curves, despite a reasonable overlap of the corresponding biased probabilities, $\mathscr{P}_{\text{bias}}(\psi)$. Because of the very slow improvement in their matching, "windows" 2 and 3 may still require considerable sampling before a satisfactory convergence is attained. It has, therefore, been decided to report only the data characterizing the transition from ‡ to the β-strand at this temperature.

Strikingly, neither the evolution of $\Delta A_{\alpha_R\to\ddagger}(T)$ nor that of $\Delta A_{\beta\to\ddagger}(T)$ is monotonic as the temperature increases. In fact, these two profiles exhibit a maximum, viz at $T_i = 340$ K for the former and at $T_i = 320$ K for the latter, as may be observed in Figure 2. The difference in the free energies characteristic of two consecutive temperatures is always greater than the total error associated to either $\Delta A_{\alpha_R\to\ddagger}$ or $\Delta A_{\beta\to\ddagger}$, thereby ruling out the possibility of a fortuitous behavior that could result from accumulated statistical and systematic errors. Consequently, the non-Arrhenius behavior witnessed in the unfolding of $AcNH_2-$

(99) Darve, E.; Pohorille, A. Calculating free energies using average force. *J. Chem. Phys.* **2001**, *115*, 9169−9183.
(100) Darve, E.; Wilson, M.; Pohorille, A. Calculating free energies using scaled-force molecular dynamics. *Mol. Simul.* **2002**, *28*, 113−144.
(101) Bartels, C.; Karplus, M. Multidimensional adaptive umbrella sampling: Applications to main chain and side chain peptide conformations. *J. Comput. Chem.* **1997**, *18*, 1450−1462.

$(\text{L-Leu})_{11}-\text{NHMe}$ at its C-terminus is not coincidental but, on the contrary, must be governed by underlying physical principles, likely to be related to the solvation properties of this hydrophobic homopolypetide.

3.2. Three-Dimensional Lattice Model Simulations. The conformation corresponding to the minimum of the free energy, obtained with a poor solvent, viz $B_s = -8.0$, is an α-helix analogue, denoted $\mathcal{A}$. This conformation, shown in Figure 1, is unique and constitutes the ground state of the free energy spectrum of the system. It features nine intrachain contacts and six α_R-type interactions. The free energy associated to $\mathcal{A}$ is given by

$$\Delta A^{\mathcal{A}}_{\text{total}}(T) = 9B^{\text{eff}}(T) + 6\epsilon_{\alpha_R} \tag{18}$$

To characterize the state of the chain, the heat capacity and the order parameter of the homopolypeptide chain were computed using a Monte Carlo (MC) algorithm.[102] The order parameter,[103] $\langle Q(T)\rangle$, of the chain is defined as the average fraction of contacts in common with conformation $\mathcal{A}$. The order parameter is 1 only if conformation $\mathcal{A}$ has a substantial probability of occurrence. It decreases toward 0 as the number of relevant structures becomes increasingly larger. In each MC simulation, the initial conformation was always $\mathcal{A}$. Next, 20 000 MC steps of relaxation were performed, followed by 100 000 MC steps to compute the statistical ensemble averages. Here, the chain is small enough to allow a rapid convergence of these averages employing a limited sampling. The evolution of the heat capacity and the order parameter with the temperature obtained for $B_s = -8.0$ and at T varying from 0.10 to 2.00 by increments of 0.05 are displayed in Figure 3. The peak in the heat capacity profile delineates well the frontier between the ordered and the disordered regions of the conformational space. Furthermore, it coincides with a sharp decrease of the order parameter. This thermodynamic characteristic arises at the folding temperature of $T_f = 0.65$. The chain is in a well-ordered state when $T < T_f$ and disorganized at larger temperatures.

One of the goals of this study is to characterize the transition between a conformation corresponding to a local minimum of the free energy landscape and conformation $\mathcal{A}$, located in the region of highly ordered structures. The conformation, referred to as $\mathcal{B}$ in Figure 1, chosen among the ensemble of compact structures, is, indeed, a local minimum of the free energy landscape. In essence, this structure is analogous to the β conformation. The difference in free energy with the extended structure is given by

$$\Delta A^{\mathcal{B}}_{\text{total}}(T) = 9B^{\text{eff}}(T) + 3\epsilon_{\alpha_R} \tag{19}$$

It is worth noting that, because the compactness, that is, the number of contacts, of $\mathcal{B}$ is equal to that of $\mathcal{A}$, the pairwise, intrachain contribution to the free energy becomes identical for both structures. The difference in free energy between these conformations arises from the helix contributions.

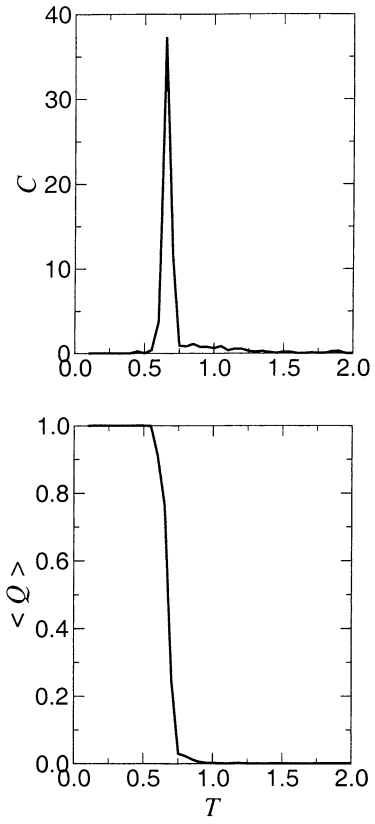

Figure 3. Heat capacity (top) and order parameter (bottom) of the homopolypeptide chain, as a function of the temperature. Here, $B_s = -8$.

For each temperature between 0.10 and T_f, by increments of 0.05, 100 MC simulations were performed to pinpoint the transition state separating $\mathcal{B}$ from $\mathcal{A}$. The starting conformation of the MC sampling was $\mathcal{B}$, and each trajectory was interrupted when $\mathcal{A}$ was reached. For each trajectory, the conformation associated to the largest free energy was determined. Among the resulting structures, that corresponding to the lowest free energy was defined as the transition state, ‡, located between $\mathcal{A}$ and $\mathcal{B}$. This transition state is the same within the range of temperatures explored. Conformations $\mathcal{C}_1$ and $\mathcal{C}_2$ along the pathway connecting $\mathcal{A}$ to $\mathcal{B}$ through ‡ are shown in Figure 1. The number of bonds formed between the last monomer and unoccupied vertexes of the lattice could be seen as an analogue of its associated SASA. By simply tallying monomer−solvent bonds in Figure 1, we find a SASA equal to 3, 5, and 2 for the $\mathcal{A}$, ‡, and $\mathcal{B}$ conformational states, respectively. It is worth underlining that the SASA($\mathcal{B}$) < SASA($\mathcal{A}$) < SASA(‡) relationship is consistent with the data obtained from classical MD simulations for the α_R, ‡, and β conformations.

The free energy difference between conformations $\mathcal{C}_1$, $\mathcal{C}_2$, ‡, and an extended structure can be expressed as

$$\begin{aligned}\Delta A^{\mathcal{C}_1}_{\text{total}}(T) &= 7B^{\text{eff}}(T) + 5\epsilon_{\alpha_R}\\ \Delta A^{\mathcal{C}_2}_{\text{total}}(T) &= 6B^{\text{eff}}(T) + 4\epsilon_{\alpha_R}\\ \Delta A^{\ddagger}_{\text{total}}(T) &= 6B^{\text{eff}}(T) + 3\epsilon_{\alpha_R}\end{aligned} \tag{20}$$

At each temperature, the free energy differences between those conformations along the pathway, viz $\mathcal{A}$, $\mathcal{C}_1$, $\mathcal{C}_2$, ‡, and $\mathcal{B}$, and $\mathcal{A}$ are reported in Figure 1. These data reveal a clear and

(102) Metropolis, N.; Rosenbluth, A. W.; Rosenbluth, M. N.; Teller, A. H.; Teller, E. Equation of state calculations by fast computing machines. *J. Chem. Phys.* **1953**, *21*, 1087−1092.
(103) Dinner, A.; Šali, A.; Karplus, M.; Shakhnovich, E. Phase diagram of a model protein derived by exhaustive enumeration of the conformation. *J. Chem. Phys.* **1994**, *101*, 1444−1451.

unambiguous temperature dependence of the free energy profiles. Furthermore, the activation free energies defined by

$$\Delta A_{\mathscr{A}\to\ddagger}(T) = -3B^{\mathrm{eff}}(T) - 3\epsilon_{\alpha_R}$$
$$\Delta A_{\mathscr{B}\to\ddagger}(T) = -3B^{\mathrm{eff}}(T) \quad (21)$$

are shown in Figure 2. They exhibit a conspicuous nonmonotonic behavior as the temperature increases. At $T_i = 0.28$, the two curves, $\Delta A_{\mathscr{A}\to\ddagger}(T)$ and $\Delta A_{\mathscr{B}\to\ddagger}(T)$, reach a maximum.

3.3. Role of the Hydrophobic Effect. As can be seen in Figures 1 and 2, classical MD free energy calculations and lattice model simulations provide a consistent answer, with a similar behavior of the free energy of activation as a function of the temperature. A qualitative analysis of the solvation thermodynamics common to the two approaches can be carried out in the light of the present results and the basic relationship connecting the entropy and the free energy changes. Focusing on the conformational change between a minimum, ξ, of the free energy landscapes, viz. ξ is either the α-helix, $\mathscr{A}$, the β-strand, or $\mathscr{B}$, and the transition state, ‡, we find the variation of entropy is $\Delta S^{\ddagger}(T) = -\partial\Delta A^{\ddagger}(T)/\partial T$. In addition, the internal energy change is expressed as $\Delta U^{\ddagger}(T) = \Delta A^{\ddagger}(T) + T\Delta S^{\ddagger}(T)$. At the temperature where $\Delta A^{\ddagger}(T)$ is maximum, that is, $T = T_i$, the entropy is zero. Because $\Delta A^{\ddagger}(T)$ decreases when $T > T_i$, it follows that $\Delta S^{\ddagger}(T)$ is positive, which, in other words, implies that the transition state is entropically favored. Considering that $\Delta A^{\ddagger}(T) > 0$, we find the change in internal energy, $\Delta U^{\ddagger}(T)$, is necessarily positive, and ξ is the energetically favored thermodynamic state. Symmetrically, at $T < T_i$, $\Delta S^{\ddagger}(T)$ is negative, and the ξ is the entropically favored state. Evolution of $\Delta U^{\ddagger}(T)$ cannot be inferred directly from the identity $\Delta A^{\ddagger}(T) = \Delta U^{\ddagger}(T) - T\Delta S^{\ddagger}(T)$. It can, however, be anticipated that, at low temperatures, the contribution of the peptide chain to the change in internal energy should be positive, because the SASA, independent of the temperature, is greater for the transition state than for ξ. Considering the greater exposure of the former to the aqueous environment, we expect the contribution of the solvent to be positive on account of the disrupted network of hydrogen bonds formed around the last residue of the homopolypeptide.

In light of the greater SASA for the transition state, the simulated conformational change from ξ to the transition state, ‡, can be viewed as the transfer of a portion of the side chain from a buried state to a solvent-exposed one. This phenomenon is similar in spirit to the transfer of a hydrophobic solute from a nonpolar medium to water, which is accompanied by the thermodynamic fingerprint of the hydrophobic effect, namely a positive free energy change.[41,42] When the results are put together, it is apparent that the internal energy and the entropy differences play distinct roles as a function of the temperature. In line with previous investigations of the hydrophobic effect, the thermodynamic origin of the free energy barrier stems, at high temperatures, from the sole internal energy, to which an increasing entropic contribution is added as the temperature is lowered.[104]

Conclusion

The reversible unfolding of a short peptide chain was investigated by means of multi-nanosecond, classical MD free energy calculations and MC three-dimensional lattice simulations as a function of the temperature. In the former, the transition of the C-terminal residue of $AcNH_2-(L\text{-}Leu)_{11}-NHMe$, from its α-helical to its β-strand conformation, was examined between 280 and 370 K, whereas, in the latter, the free energy barrier separating the analogues of an α-helix and a β-strand of a nonpolar, twelve-residue homopolypeptide was determined over a sufficiently large range of temperatures. The positive value of the activation free energy found in this work corresponds to the thermodynamic signature of the hydrophobic effect. The consistent picture provided by the two alternative approaches reveals a non-Arrhenius behavior in the unfolding kinetics, characterized by a maximum of the free energy along the transition pathway at an intermediate temperature within the range of values explored. The nonmonotonic evolution of the free energy as the temperature increases is a manifestation of the competition between internal energy and entropy contributions. As has been discussed amply,[41,42,104] the hydrophobic effect stems from the loss of internal energy at high temperature, when the peptide chain is exposed toward the solvent. At low temperature, the entropy also contributes to hinder the unfolding of the homopolypeptide. The remarkable agreement between the results obtained with classical MD and lattice model simulations magnifies the importance of temperature-dependent effective potentials in coarse-grained approaches targeted at modeling the folding/unfolding process of a peptide over a range of temperatures.

Acknowledgment. The authors would like to thank Andrew Pohorille, Eugene Shakhnovich, Hue-Sun Shan, Themis Lazaridis, and Jérôme Delhommelle for fruitful discussions and insightful suggestions to improve the manuscript. Preliminary results of this work were presented at a CECAM workshop in Lyon, France, in May 2002. The Centre Charles Hermite (CCH), Vandœuvre-lès-Nancy, France, and the CINES, Montpellier, France, are gratefully acknowledged for provision of generous amounts of CPU time on their SGI Origin 2000 and Origin 3800.

JA029075O

(104) Southall, N. T.; Dill, K. A. The mechanism of hydrophobic solvation depends on solute radius. *J. Phys. Chem. B* **2000**, *104*, 1326−1331.